Title

Dimerization dependent fluorescent protein biosensor for characterizing regulatory protein caging system for chimeric antigen receptors.

Author

Mathew, Angel

Publication Date

2021

Peer reviewed|Thesis/dissertation

UNIVERSITY OF CALIFORNIA SAN DIEGO

Dimerization dependent fluorescent protein biosensor for characterizing regulatory protein caging system for chimeric antigen receptors.

A Thesis submitted in partial satisfaction of the requirements for the degree

Master of Science

in

Bioengineering

by

Angel Mathew

Committee in charge:

Professor Yingxiao Wang, Chair
Professor Geert W. Schmid-Schönbein
Professor Lingyan Shi

2021

The thesis of Angel Mathew is approved, and it is acceptable in quality and form for publication on microfilm and electronically.

University of California San Diego

2021

TABLE OF CONTENTS

LIST OF FIGURES

ACKNOWLEDGEMENT

I would like to acknowledge Dr. Yingxiao Wang for his invaluable guidance and support as the chair of my committee. Also, I would like to acknowledge Dr. Reed Harrison and other members of the lab who have laid the foundation of this project. I am grateful for their help and patience in guiding me with various aspects of my thesis.

ABSTRACT OF THE THESIS

Dimerization dependent fluorescent protein biosensor for characterizing regulatory protein caging system for chimeric antigen receptors.

by

Angel Mathew

Master of Science Bioengineering

University of California San Diego, 2021

Professor Yingxiao Wang, Chair

Chimeric antigen receptor (CAR)-T cell therapies have adverse side effects such as cytokine release syndrome (CRS) due to on-target off-tumor toxicity. Responses for clinically available CAR-T therapies mainly use immunosuppressants for mitigation which lowers their overall functionality. An alternate approach will be to bioengineer cellular regulation that confers high spatiotemporal control over CAR-T cells in vivo to reduce its side effects. The lab has

previously developed a protein caging system as a switch for controlling the signalling of CAR. The caging domain binds to CAR and keeps it auto inhibited. The uncaging domain which is under an external control can bind to the caging domain and free the CAR to initiate intracellular signaling. We have tested two strategies for externally controlling the uncaging of CAR by creating a dihydrofolate reductase (DHFR) system and a heat shock promoter (HSP) system. We have developed an in-vitro dimerization dependent fluorescent (ddFP) biosensor that can detect dynamics of the above protein caging system by verifying the expression and binding of the caging and uncaging domains. The results can be used to further optimize the protein caging system and create focused ultrasound (FUS) controllable CAR-T cell

CHAPTER 1. BACKGROUND

1.1.CAR-T immunotherapy and regulation of CRS

Recent advances in immunotherapy have been successful in obtaining high remission rates in cancer patients with advanced B cell cancer. One of the most powerful forms of immunotherapy is known as chimeric antigen receptor (CAR) T cell therapy. FDA has approved the use of second-generation CD19-directed CAR T cells (CAR-CD19), i.e. tisagenlecleucel and axicabtagene ciloleucel for the treatment of Acute Lymphocytic Leukemia (ALL) and Non-Hodgkin Lymphoma (NHL). [1][2]

However one of the major challenges that limits the wide scale application of CAR-T therapy is potentially life threatening side effects due to lack of control over infused CAR-T cells. CAR T cells are capable of rapid proliferation and activation inside the body releasing large amounts of pro-inflammatory cytokines. As result the most common side effect of CAR-T therapy is cytokine release syndrome (CRS); a systemic inflammatory response leading to high fever, hypotension and hypoxia. Depending on the severity of tumor burden, CRS can range from mild fever to severe organ dysfunction [3]. Targeting tumor antigen is also problematic as most antigens expressed on tumors are also found in low levels on healthy cells. This leads to on-target off-tumor toxicities which further hampers the development of CAR-T cell therapies for solid tumors. These side effects are currently mitigated using immuno suppressants for IL-6 which drastically reduces the time span of functional CAR T cells. Hence, there is a dire need to develop controllable CAR designs [4]. Several regulatory mechanisms such as light inducible

CAR-T, drug inducible CAR-T, multiple antigen targets, suicide/protein based switches have been researched [5].

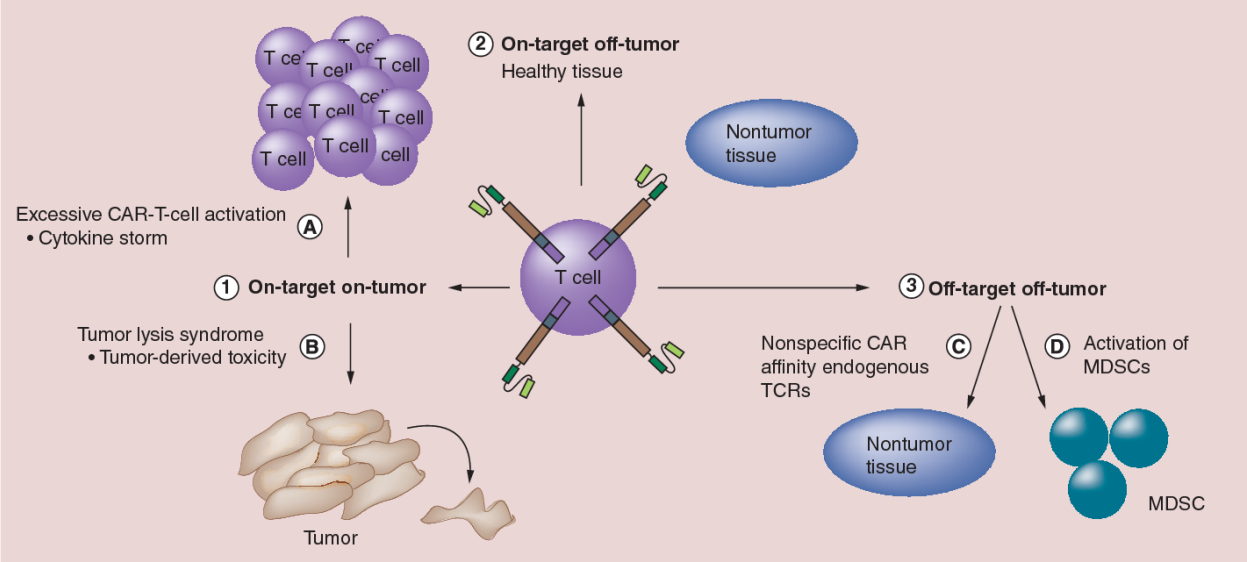

Figure 1: Diagram showing different modes of CAR-T induced toxicity in the body[3]

In our lab we are using focused ultrasound stimulation (FUS) for high spatiotemporal activation of CAR T cells with precision control directly over the tumor. Focused ultrasound can penetrate centimeters deep into the tissue and noninvasively induce heat and mechanical stress. Development of a Boolean gated acoustogenetic CAR that is activated in the presence of external FUS can drastically reduce the on-target off-tumor toxicity. We can also achieve significant homing, improved persistence, and less T cell exhaustion resulting in a safer and more efficient treatment for patients.

1.2 Boolean gate controlled CAR using protein caging system

CARs are synthetic receptors derived from T cell receptors (TCR) [6]. However CARs don't need tumor antigens to be presented by MHC. Instead they contain an extracellular single

chain variable fragment region (scFv) for recognising and binding to tumor antigens. There is also a transmembrane domain that acts like a flexible hinge region. The intracellular part has multiple ITAM signal transduction domain of CD3-zeta chain (CD3ζ) [7]. Recognition of antigen by scFv induces catalytic activation of Src family kinases. These kinases phosphorylates tyrosine residues on ITAMs which has increased binding affinity towards ZAP-70. Subsequent phosphorylation of ZAP-70 by ITAM results in a signalling cascade leading to T cell activation and its effector functions of releasing cytokines [8]. In second and third generation CARs there is also an additional intracellular region containing one or more costimulatory domains such as CD28 or OX40 regions. These co-stimulatory regions contribute to expansion, cytokine secretion and other antitumor activity [9].

From the earlier research conducted in the lab, a standard D23 CAR design was created by modification of a second generation CAR. In this modification, multiple ITAMs were removed and only a single ITAM1 was utilized. The main aim was to reduce the number of ITAMs to a single ITAM which could be easily caged using our protein caging strategy. Recent research from the Sadelain group suggested that a single ITAM may be sufficient for a strong T cell response [10]. The lab had previously modified D23 CAR to be auto inhibited by using a protein domain, Nef, that binds to ITAM. It was previously shown that binding of Nef prevents phosphorylation of ITAM [15]. We hypothesis that ITAM's subsequent interactions with Zap70 will be affected resulting in no T cell activation. This CAR design was called D23-Nef. A boolean gate system was used to induce the expression of a synthetically developed ITAM variant (Decoy1) which would free the caged ITAM by binding to Nef. Final structure of this CAR was composed of a single chain variable fragment(scFv) targeting CD19, a CD28 domain

spanning from the extracellular space to the cytoplasmic space, a single ITAM1 from CD3ζ, and EV linker and a C terminal Nef caging domain.

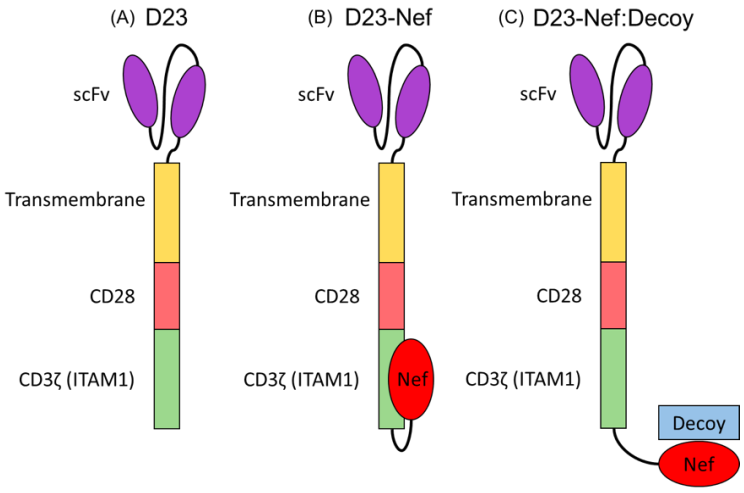

Figure 2: (A) Standard D23 CAR (B) D23-Nef contains the caging domain (C) D23-Nef-Decoy1 represents the uncaged CAR

Initial in vitro assays have verified this binding between ITAM and Nef as well as Nef and Decoy1. In the uncaged state, the D23-Nef CAR can bind to CD19 antigen on tumor cells and induce a cytotoxic response. Hypothetically, D23-Nef CAR also has an additional advantage of increased homing to the tumor in it's caged form. Hence, after the subsequent uncaging of the CAR there should be an improved cytotoxic response along with lesser on target off tumor toxicity.

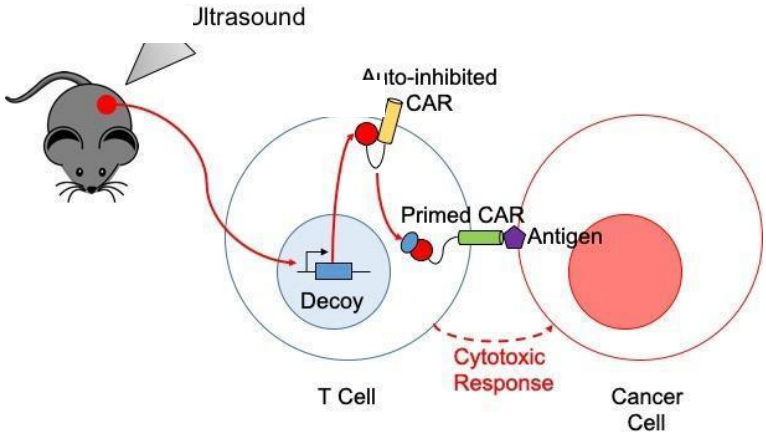

Figure 3: Schematic representation of FUS induced activation of autoinhibited CAR containing the protein caging system

1.3. Principle of assay development using dimerization dependent fluorescent protein biosensor

Dimerization dependent fluorescent protein (ddFP) technology developed by Campbell's group can be used as a qualitative biosensor to measure interactions between two different proteins [11]. The ddFP consists of a pair of FP. One of the monomers in the ddFP pair contains a chromophore (copy A) and the other monomer is non fluorescent (copy B). When they are separate there is a dim basal level of fluorescence from copy A. Heterodimerization of copy A with copy B results in an increase in the fluorescence brightness. A fluorescent protein exchange (FPX) strategy has been recently developed using two pairs of ddFP [12]. Here there will be two copy A monomers and they swap the same copy B depending on protein protein interactions resulting in changing colors.

The goal of our ddFP biosensor was to develop a FPX live cell imaging assay to study the dynamics of our protein caging system following an external stimulation. We tested out two different strategies for developing a boolean gated uncaging by Decoy1. In our first strategy, our objective was to create a highly unstable Decoy1 which was degraded rapidly by the cell but could only be stabilized in the presence of a drug. Our second strategy was to induce the expression of Decoy1 only after the cell has been stimulated with heat shock. Here, we use two monomers, GA derived from GFP and RA derived from dtomato as the two copy A in our FPX strategy. In the monomeric state they have a dim fluorescence in green and red channels respectively. Their fluorescence intensity increases only after dimerizing with the copy B monomer, B3 [12].

We created constructs by tagging fluorescent monomers GA and RA with ITAM and Nef. We tagged ITAM with the quenched fluorescent monomer GA through a 34 mer linker forming ITAM-GA. Similarly we tagged the uncaging domain, Decoy1 with the quenched fluorescent

monomer RA (Decoy1-RA). Caging domain Nef was directly attached to B3 (Nef-B3), and we hypothesized that in the caged state our live cell imaging assay would have high green fluorescence from GA:B3 and in uncaged state it would have a high red fluorescence from RA:B3.

For our drug dependent boolean gated uncaging system, we created a fusion protein system, where Decoy1-RA was fused through a linker with an unstable protein, dihydrofolate reductase (DHFR). This unstable protein, DHFR conferred its instability to Decoy1-RA resulting in rapid degradation.[13] Addition of a small-molecule ligand trimethoprim (TMP) stabilizes the destabilizing domain. In the stable form, Decoy1-RA can bind to Nef and uncage ITAM. This strategy is henceforth called the DHFR system.

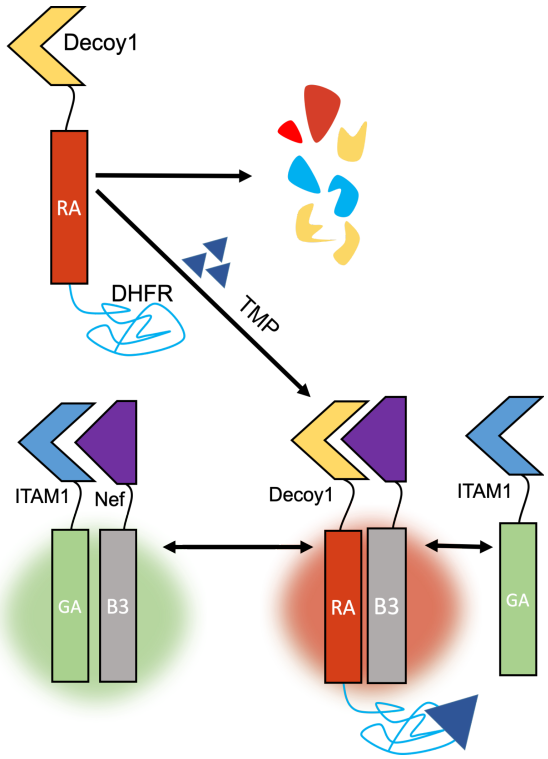

Figure 4: Schematic representation of drug induced boolean gated uncaging of protein caging system (DHFR system)

In our second strategy, our objective was to induce the expression of Decoy1-RA only after the cell has been stimulated with heat shock. This was achieved by using a heat shock promoter, HSP70-P for inducing the expression of Decoy1-RA following a heat shock [14]. We hypothesized that after the heat shock induced expression, Decoy1-RA can immediately uncage ITAM by binding to Nef. This strategy is henceforth called the HSP system.

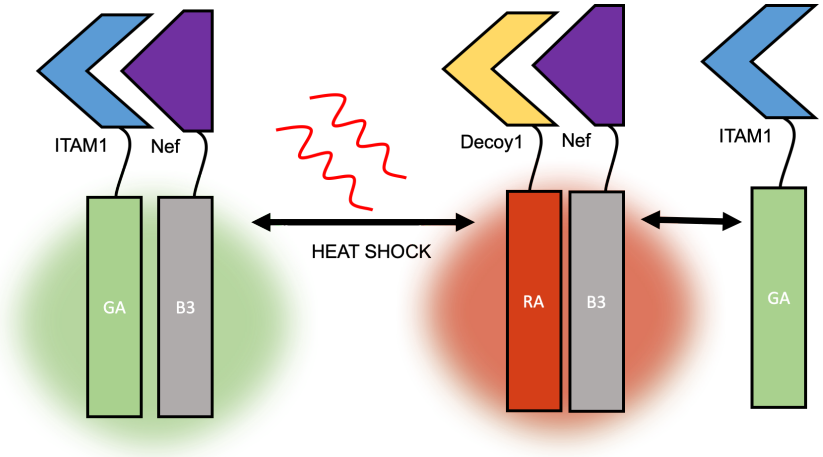

Figure 5: Schematic representation of heat shock induced boolean gated uncaging of protein caging system (HSP system)

CHAPTER 2. RESULTS

2.1. Construction of ddFP biosensor for characterizing protein caging dynamics in a DHFR system

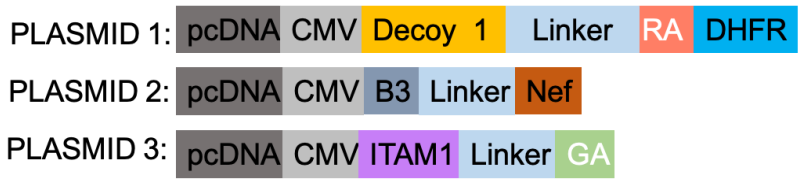

Figure 6: Constructs design of ddFP biosensor for DHFR System

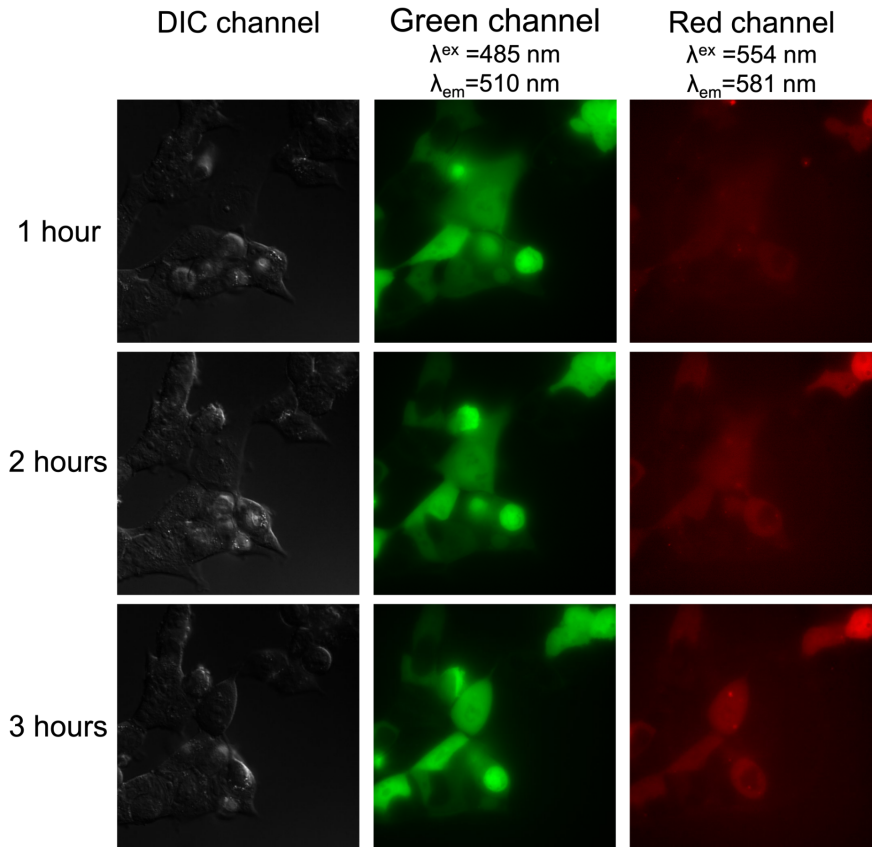

Figure 7: Micrographs of time lapse fluorescent imaging of position 12 from DHFR system showing DIC, Green fluorescence from GA and red fluorescence from RA at 1,2,3 hours.

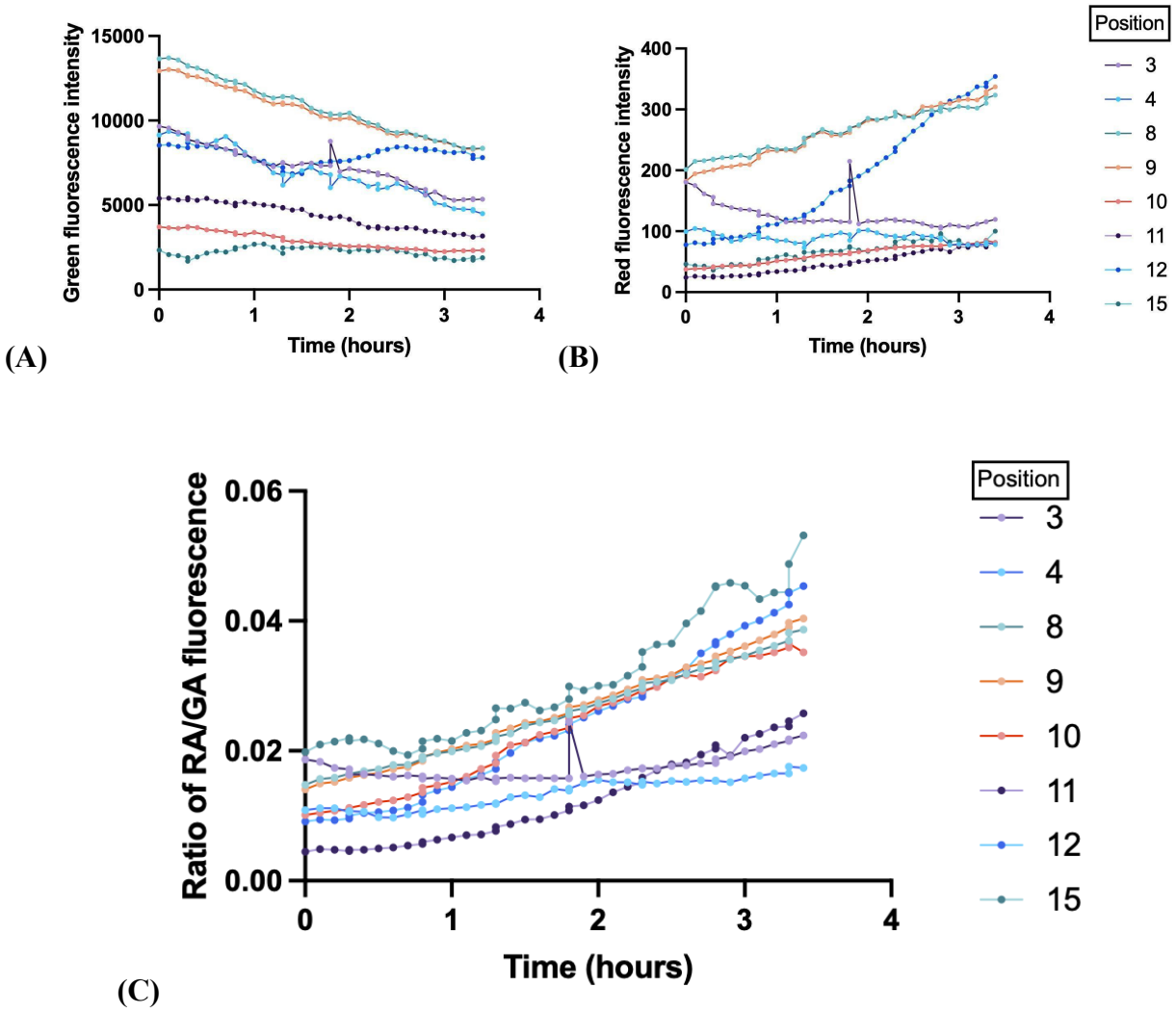

Figure 8: Intensity vs time graphs of (A) Green fluorescence channel and (B) Red fluorescence channel from time lapse microscopy of 8 different positions for 3.5 hours. (C) Red by green ratio vs time for cells at 8 different positions for 3.5 hours

In order to test the ddFP biosensor to observe protein uncaging in DHFR systems we constructed plasmids in figure 6 and transfected HEK293T cells as described in the materials and methods. After adding 1μm of TMP to the system, we performed a time lapse microscopy over a course of 3.5 hours for 16 stage positions. In figure 7 micrographs from cells at the stage position 12 visually compare the fluorescence emitted by the cells in green channel and red channel.

Figure 8A shows green fluorescence intensity emitted by chosen stage positions visibly declining over a period of 3 hours. As expected there is a corresponding increase in the red fluorescence intensity emitted by cells at various stage positions during the next 3.5 hours in figure 8B. Plotting the ratio of red fluorescence by green fluorescence in figure 8C demonstrates clearly that after addition of TMP, it takes about 1 hour to see a noticeable rise in the red fluorescence and decline in green fluorescence. This is shown by the 95% confidence interval, r =(-0.9987, -0.9996), p <0.0001. This shift from green to red fluorescence supports our hypothesis that TMP stabilizes Decoy1, which shifts the dynamics of the protein caging system from caged to uncaged mode.

2.2. Construction of ddFP biosensor for characterizing protein caging dynamics in the HSP system

(A)

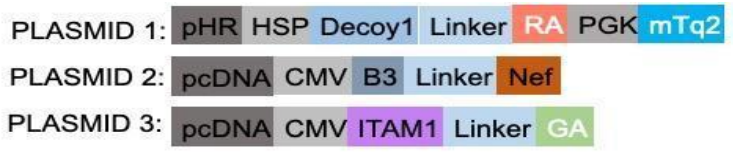

(B)

Samples	Plasmids	Heat shock (T=0 hr)	Expected Emission channels
Test	1,2,3	No	Green, Cyan
Test	1,2,3	Yes	Green, Red, Cyan
Uncaged control	1,2	Yes	Red, Cyan
Caged control	2,3	Yes	Green

Figure 9: (A) Construct design of ddFP biosensor for HSP system (B) Tabular representation of samples, constructs, heat shock status and expected emission channels.

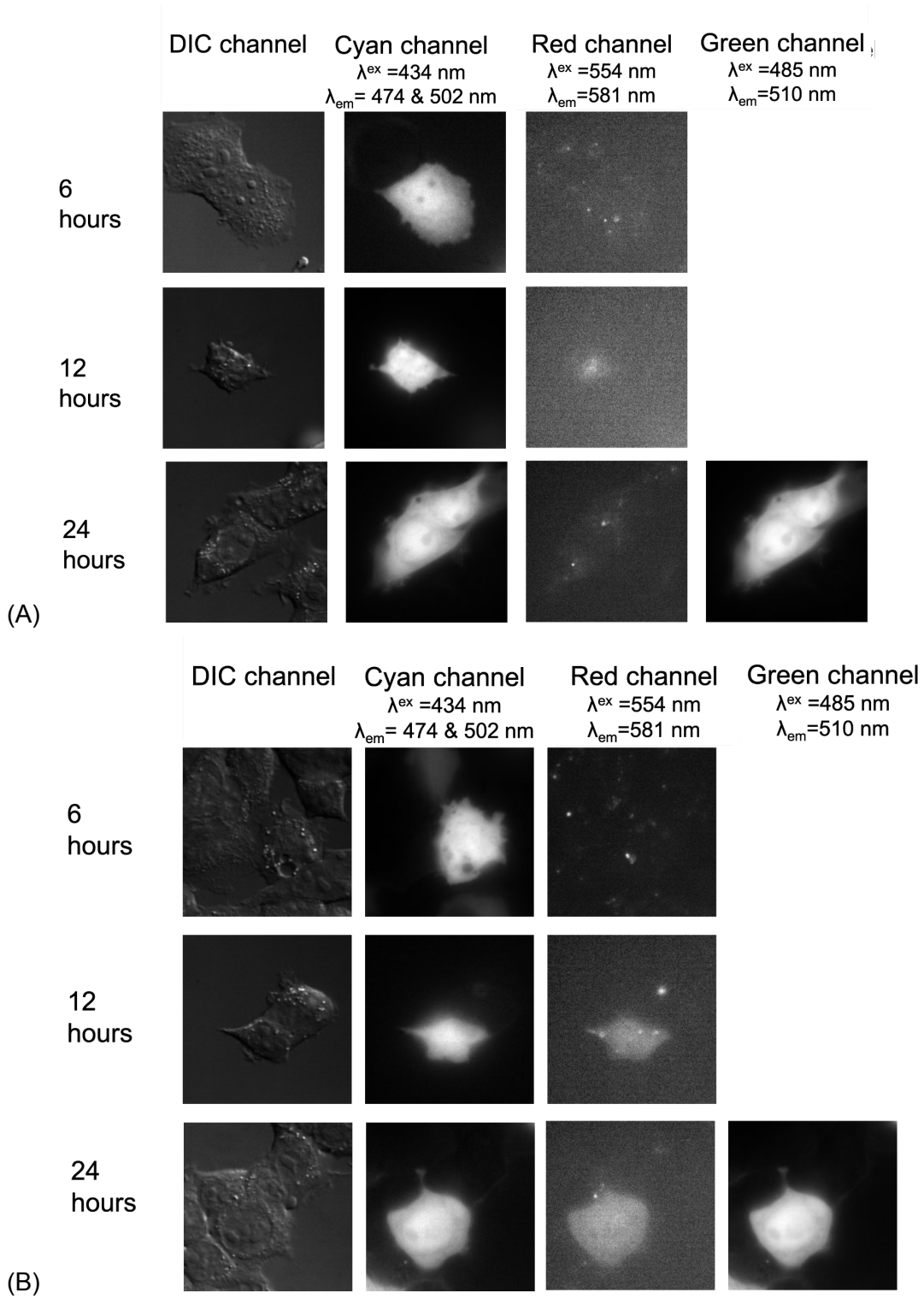

Figure 10: Micrographs of fluorescent imaging at 6,12 and 24 hours time points for DIC, cyan channel for mTq2, red channel for RA and green channel for GA (A) Test with plasmids 1,2,3,HS- (B) Test with plasmids 1,2,3,HS+ (C) Uncaged control with plasmids 1,2,HS+ and (D) Caged control with plasmids 2,3,HS+.

Figure 10: continued

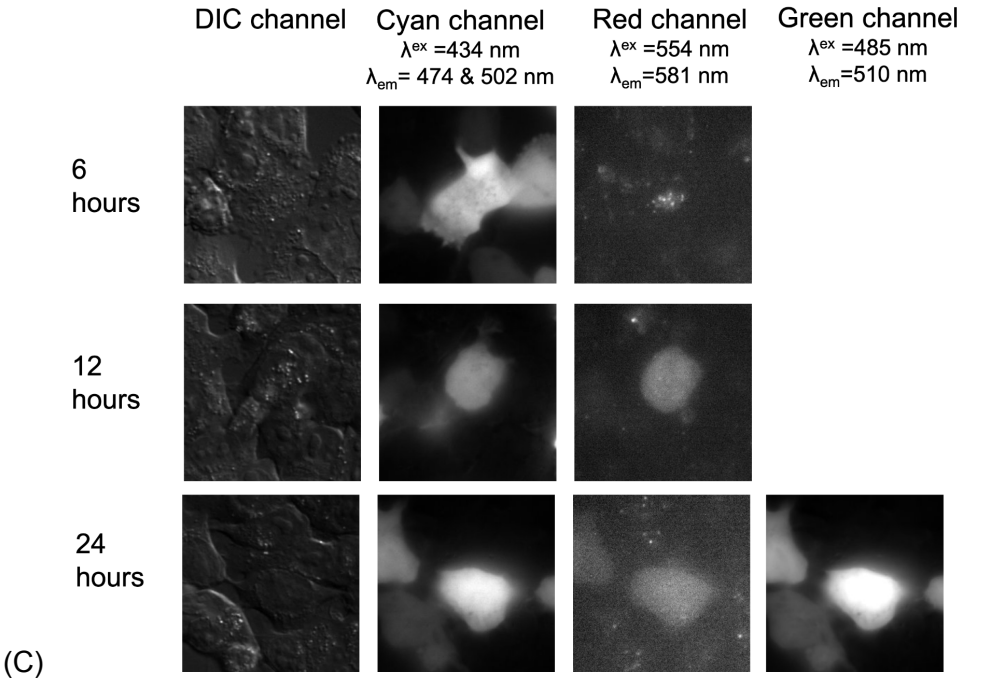

(C)

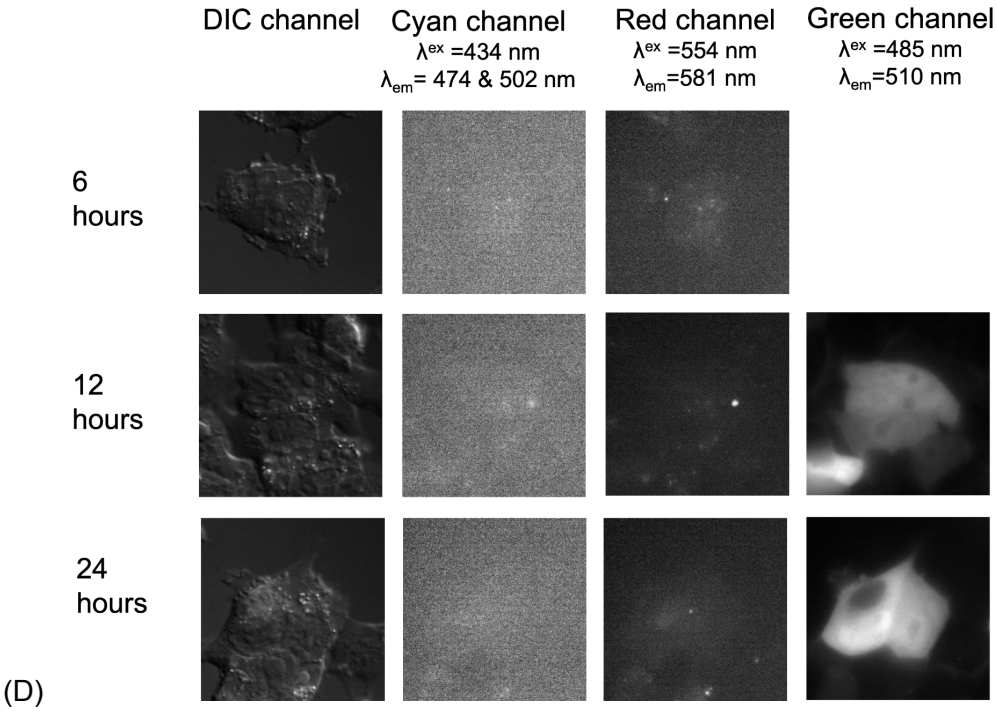

(D)

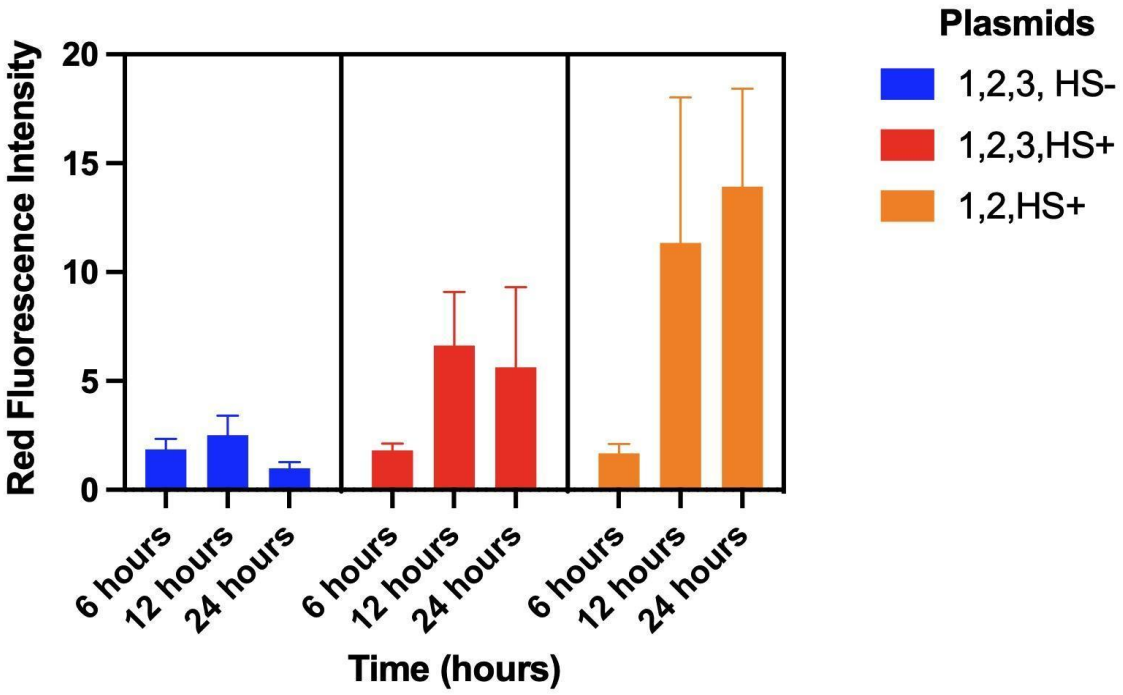

Figure 11: Red fluorescence intensity vs time graph at 6,12,24 hour time points for test (1,2,3, HS-), test (1,2,3, HS+) and uncaged control (1,2 HS+)

The results from testing the ddFP DHFR system gave us low contrast between the green and red channels. We hypothesized that this might be due to a low rate of degradation of DHFR which resulted in degradation of the decoy1-RA system leading to low levels of red fluorescence. We decided to follow an alternative strategy of using a heat shock promoter to induce expression of Decoy1-RA. We also decided to include another fluorophore mTq2 within the Decoy1-RA plasmid under a constitutively expressing PGK promoter inorder to identify cells that were transfected with plasmid 1 for imaging at 6 hour time points. Figure 9A gives the construct design for HSP systems. Samples were prepared using different combinations of plasmids. We decided to prepare two samples with all the constructs of the protein caging system and then look at the dynamics of caging and uncaging, with and without heat shock. We also created two samples to act as caging control and uncaging control as they only had a

combination of 2 components necessary for their function. We decided to gather the fluorescence from 3 channels green, red and cyan for capturing fluorescence emitted from GA, RA, and mTq2 respectively as described in the figure 9B. The plasmid was constructed and cells were transfected and prepared as described in the materials and methods section. After performing heat shock, cells were incubated for 6 hours before imaging. Micrographs from different samples were obtained at three different time points (6, 12 and 24 hours). Figure 10A shows a micrograph of Test which contains plasmids 1,2,3 with no heat shock. We hypothesized that this sample would only result in a green fluorescence and very minimal levels of fluorescence in the red channel at all time points. For imaging, cells showing emission in the cyan channel indicating presence of plasmid 1 which contained RA-Decoy1 were chosen. It is clearly visible that without heat shock there is only a basal level of autofluorescence in the Red channel at all time points. Next we investigated the fluorescence emitted by test + HS sample which contains plasmids 1,2,3 required for a complete protein caging system figure 10B. After heat shock, when the dish was imaged at 6 hours there is only a basal level of autofluorescence in the red channel. However, there is an increasing level of red fluorescence in this sample at time points 12 and 24 hours. This verifies our hypothesis that RA-Decoy1 is only expressed after heat shock. Micrographs from our uncaged control sample in figure 10C, shows a similar fluorescent profile to Test + HS sample. Micrographs from caging control figure 10D is similar to the micrograph from Test with no heat shock as it shows no fluorescence in the red channel.

Figure 11 shows the red fluorescence intensity emitted from all the stage positions scanned from two Test (with and without heat shock) and uncaged control. There is a basal level of red fluorescence in all three samples at the initial time point of 6 hours. This is because at this time, the hsp70 induced expression is slow resulting in a low rate of uncaging. And there is

autofluorescence in the red channel. However, at 12 and 24 hour time points, we can see an increase in the uncaging domain shown by increasing red fluorescence intensity with respect to basal level of red fluorescence in Test without heat shock at the corresponding time points.

CHAPTER 3. DISCUSSION

Regulation of CAR is important in CAR-T cell therapy to curb it's side effects such as CRS and make it a safer treatment [5]. CRS progresses from stage 1 to stage 3 which shows increasing severity. Severity depends on tumor burden, peak number of CAR-T, lymphodepletion etc. Stage 1 is characterized by CAR-T cell expansion and mild local inflammation at the tumor. However stage 3 is caused due to CAR-T cell redistribution and its on target off tumor activity [17]. This is the most critical stage which can cause organ dysfunction and ultimately the death of the patient. Currently, CRS is mitigated using pharmacological immunosuppressants such as tocilizumab to target IL-6 receptors [16]. But this reduces the efficiency of CAR-T treatment resulting in lower remission rates in patients. Thus, inducible regulation which can externally control the activation of CAR and limit its activity to tumor regions can drastically delay the progression of CRS.

In our lab we have developed a protein caging system to physically block the ITAM using a caging domain. This results in controlled regulation of T cell activation through the ITAM phosphorylated Zap70 pathway. The caged ITAM is only uncaged in the presence of an uncaging domain. Thus, a biosensor that can verify the caging and uncaging of these protein caging system in live cells will be helpful in selecting the most efficient variant of the uncaging domain.

In our surrogate system of HEK293T cells, our ddFP biosensor was able to verify the protein caging dynamics from an externally controlled induction of uncaging domain. For the DHFR system in which the uncaging domain was stabilized after addition of TMP we saw an increase in the red fluorescence and decrease in green fluorescence over a course of 3.5 hours. This showed that our ddFP biosensor for DHFR system is successful in detecting the levels of uncaging and caging domains respectively. However the red fluorescence intensity emitted by

our ddFP biosensor ranges between 0-400 arbitrary units of intensity whereas green fluorescence intensity ranges from 0-15000 arbitrary units. This might be due to the slow acting nature of stabilizing the uncaging domain resulting in lower contrast between green and red fluorescent channels. Future experiments will focus on optimizing the contrast between different channels.

In our second strategy we created a system to externally control the expression of the uncaging domain through a heat shock promoter. Following the heat shock cycle, our inducible system expressed Decoy1-RA which resulted in detectable red fluorescence after 12 hours in Test (1,2,3+HS) and uncaged control . HSP70-P is a fast acting promoter, however in our system the red fluorescence was detected at 12 hours. One possible explanation for this delay in expression can be due to the length of our long fusion protein Decoy1-RA which takes longer time to be translated. Our assay also verified the binding between the caging protein Nef and uncaging protein, Decoy1 as the ddFP system requires dimerization between Nef-B3 and Decoy1- RA to emit red fluorescence.[12] Also this can be another possible explanation for the late detection of red fluorescence after heat shock. However we also noticed that there is a significant level of autofluorescence captured in the red fluorescent channel from Dish A and Dish D at all time points. Future experiments will focus on collecting data from a larger population and eliminating the noise generated by autofluorescence from control dishes. We will also have to optimize the contrast between different channels.

Our ddFP biosensor provides proof of concept for the DHFR and HSP protein caging system to externally regulate the uncaging of D23-Nef CAR. For the future directions, additional decoy variants need to be generated through directed evolution and tested for their binding affinity for Nef to uncage the CAR.

CHAPTER 4. MATERIALS AND METHOD

Plasmids:

Initially all the fragments were amplified using PCR reaction with Q5 polymerase. Cloning strategies used NEB Gibson Assembly cloning kit. The plasmid constructs were transformed into DH5a NEBstable competent E. coli cells for amplifying DNA. Colony PCR was performed to isolate colonies with full constructs. DNA was extracted using Sigma-Aldrich GenEluteTM Plasmid Miniprep kit and constructs were verified by Sanger sequencing. Plasmids (1) pcDNA-B3-34merLinker-Nef and (2) pcDNA-kozak-ITAM1-34merLinker-GA were used for both ddFP biosensors DHFR and HSP boolean gated protein caging systems.

(3) pcDNA-kozak-Decoy1-32merLinker-RA-DHFR was used for DHFR ddFP and (4) pHR_ HSP- kozak- Decoy1 -RA_ PGK-mTurquoise2 for HSP ddFP.

Cell culture:

Maintenance of HEK293T

HEK 293T cells were cultured in DMEM (Gibco, 11995115) with 10% FBS (Gibco, 10438026) and 1% Penicillin-Streptomycin (Gibco, 15140122). They were incubated in 37°C in a 5% CO2 and 95% humidified incubator.

Transfection for DHFR system.

On a 35mm dish, 750k cells were seeded and incubated in 37°C in a 5% CO2 and 95% humidified incubator. After 24 hours when the cells reached 70% confluency , Lipofectamine 3000 (Sigma-Aldrich) kit was used to perform transient transformation using 750 ng of each plasmid 1,2,3.

Transfection for HSP system.

On a 35mm dish, 900k cells were seeded and incubated in 37°C in a 5% CO2 and 95% humidified incubator. After 24 hours when the cells reached 70% confluency , Lipofectamine 3000 (Sigma-Aldrich) kit was used to perform transient transformation using 1500 ng of each plasmid 1,2,4.

Preparation of DHFR system cells for imaging

After 24 hours, cells were trypsinized and plated on Fibronectin coated glass bottom dishes and incubated for 30 minutes followed by replacing the media with FluoroBrite DMEM media (Gibco). They were incubated for a period of 24 hours before performing time lapse imaging. 3 hours prior to imaging, 1 uM TMP was added to the cells and kept in the incubator.

Preparation of HSP system cells for imaging

After 24 hours, cells were trypsinized and 50 ul was treated with heat shock in the thermocycler with 3 cycles of 5 minute heating at 43 ˚C followed by 1 minute of cooling at 37˚C . The cells were plated on Fibronectin coated glass bottom dishes and incubated for 30 minutes followed by replacing the media with FluoroBrite DMEM media (Gibco).

Imaging acquisition and analysis:

Nikon Eclipse Ti inverted microscope installed with a 300 W Xenon lamp (Atlas Specialty Lighting), an electron multiplying (EM) CCD camera (QuantEM:512SC, Photometrics), and 100x, 40x and 10x DIC Nikon microscope objectives were used to capture all imaging data with the MetaMorph software (Molecular Devices). Image analysis of acquired images was performed using Python package, ImageJ and GraphPad Prism to calculate the fluorescence intensity from each image.

Imaging DHFR system:

In order to capture the dynamics of protein caging system 3 different channels DIC, GFP channel with a GFP-Long pass filter, mCherry channel with TxRed filter were setup in Metamorph for the time lapse imaging of DHFR system at the intervals of 5 mins for 3.5 hours.

Imaging HSP system:

In order to capture the dynamics of protein caging system 4 different channels DIC, GFP channel with a GFP-Long pass filter, mCherry channel with TxRed filter and mTurquoise2 (mTq2) channel with 455 Long pass filter were used. Both GFP and mCherry had all open excitation but mTq2 had only 420/40 nm excitation spectrum. Images were acquired using Metamorph software following 6 hours, 12 hours and 24 hours after performing the heat shock.

REFERENCES

1. V. Prasad, “Tisagenlecleucel — the first approved CAR-T-cell therapy: implications for payers and policy makers,” *Nature Reviews Clinical Oncology*, vol. 15, no. 1, Art. no. 1, Jan. 2018, doi: 10.1038/nrclinonc.2017.156.

2. S. S. Neelapu, F. L. Locke, N.L. Barlette, “Axicabtagene Ciloleucel CAR T-Cell Therapy in Refractory Large B-Cell Lymphoma,” N Engl J Med, vol. 377, no. 26, pp. 2531–2544, Dec. 2017, doi: 10.1056/NEJMoa1707447.

3. M. Kalaitsidou, G. Kueberuwa, A. Schütt, and D. E. Gilham, “CAR T-cell therapy: toxicity and the relevance of preclinical models,” *Immunotherapy*, vol. 7, no. 5, pp. 487–497, 2015, doi: 10.2217/imt.14.123.

4. T. Kishimoto, “IL-6: from arthritis to CAR-T-cell therapy and COVID-19,” *International Immunology*, no. dxab011, Mar. 2021, doi: 10.1093/intimm/dxab011.

5. L. J. B. Brandt, M. B. Barnkob, Y. S. Michaels, J. Heiselberg, and T. Barington, “Emerging Approaches for Regulation and Control of CAR T Cells: A Mini Review,” *Front. Immunol.*, vol. 11, 2020, doi: 10.3389/fimmu.2020.00326.

6. S. Yu, A. Li, Q. Liu, T. Li, “Chimeric antigen receptor T cells: a novel therapy for solid tumors,” J Hematol Oncol, vol. 10, no. 1, p. 78, Dec. 2017, doi: 10.1186/s13045-017-0444-9.

7. T. Brocker and K. Karjalainen, "Signals through T cell receptor-zeta chain alone are insufficient to prime resting T lymphocytes.", Journal of Experimental Medicine, vol. 181, no. 5, pp. 1653-1659, 1995. Available: 10.1084/jem.181.5.1653.

8. H. Wang, T.A. Kadlecek, B. B. Au-Yeung, "ZAP-70: An Essential Kinase in T-cell Signaling", Cold Spring Harbor Perspectives in Biology, vol. 2, no. 5, pp. a002279-a002279, 2010. Available: 10.1101/cshperspect.a002279.

9. H. M. Finney, A. N. Akbar, and A. D. G. Lawson, “Activation of resting human primary T cells with chimeric receptors: costimulation from CD28, inducible costimulator, CD134, and CD137 in series with signals from the TCR zeta chain,” *J Immunol*, vol. 172, no. 1, pp. 104–113, Jan. 2004, doi: 10.4049/jimmunol.172.1.104.

10. C. H. June and M. Sadelain, “Chimeric Antigen Receptor Therapy,” *N Engl J Med*, vol. 379, no. 1, pp. 64–73, Jul. 2018, doi: 10.1056/NEJMra1706169.

11. S. Alford, A. Abdelfattah, Y. Ding and R. Campbell, "A Fluorogenic Red Fluorescent Protein Heterodimer", Chemistry & Biology, vol. 19, no. 3, pp. 353-360, 2012. Available: 10.1016/j.chembiol.2012.01.006.dimer

12. Y. Ding, J. Li, J.R. Entertina, Y. Shen, I. Zhang, P.H. Tewson, C.H.G Mo, “Ratiometric biosensors based on dimerization-dependent fluorescent protein exchange,” *Nature Methods*, vol. 12, no. 3, Art. no. 3, Mar. 2015, doi: 10.1038/nmeth.3261.

13. M. Iwamoto, T. Björklund, C. Lundberg, D. Kirik, and T. J. Wandless, “A general chemical method to regulate protein stability in the mammalian central nervous system,” *Chem Biol*, vol. 17, no. 9, pp. 981–988, Sep. 2010, doi: 10.1016/j.chembiol.2010.07.009.

14. B. Bettencourt, C. Hogan, M. Nimali and B. Drohan, "Inducible and constitutive heat shock gene expression responds to modification of Hsp70 copy number in Drosophila melanogaster but does not compensate for loss of thermotolerance in Hsp70null flies", BMC Biology, vol. 6, no. 1, 2008. Available: 10.1186/1741-7007-6-5.

15. W. M. Kim, A. B. Sigalov, and L. J. Stern, “Pseudo-merohedral twinning and noncrystallographic symmetry in orthorhombic crystals of SIVmac239 Nef core domain bound to different-length TCRζ fragments,” *Acta Crystallogr D Biol Crystallogr*, vol. 66, no. Pt 2, pp. 163–175, Feb. 2010, doi: 10.1107/S090744490904880X

16. B. Caulier, J. Enserink and S. Wälchli, "Pharmacologic Control of CAR T Cells", *International Journal of Molecular Sciences*, vol. 22, no. 9, p. 4320, 2021. Available: 10.3390/ijms22094320.

17. C. Bonifant, H. Jackson, R. Brentjens and K. Curran, "Toxicity and management in CAR T-cell therapy", *Molecular Therapy - Oncolytics*, vol. 3, p. 16011, 2016. Available: 10.1038/mto.2016.11.